

# Higher-order variational finite difference schemes for solving 3-D paraxial wave equations using splitting techniques

Eliane Bécache\*, Francis Collino, Patrick Joly

*INRIA, Domaine de Voluceau-Rocquencourt, BP 105, F-78153 Le Chesnay Cédex, Paris, France*

Received 23 November 1998; received in revised form 19 July 1999

---

## Abstract

Numerical schemes for solving 3-D paraxial equations are constructed using splitting techniques. The solution can be reduced to a series of 2-D paraxial equations in each direction of splitting. The discretization along the depth is based on higher-order conservative schemes. The discretization along the transverse variables is based on higher-order finite difference variational schemes. Numerical experiments illustrate the advantages of higher-order schemes, which are much less dispersive, even for a small number of discretization points per wavelength. ©2000 Elsevier Science B.V. All rights reserved.

---

## 1. Introduction

Paraxial approximations of the wave equation are commonly used when waves propagate in directions close to a preferred direction, which plays the role of an evolution variable. The operator in the Helmholtz equation is expressed as the product of two one-way operators that involve the square root of an operator. The nonlocal operator square root is then approximated to obtain a local parabolic partial differential equation. Accuracy depends on the magnitude of the error in the approximation; wider propagation angles are permitted with better approximations. Several approximations have been designed, such as the 15, 45, and 60° approximations [1]. One of the main applications of paraxial approximations is to range-dependent ocean acoustic propagation problems, where the range is the evolution variable. Tappert's parabolic equation was the first paraxial approximation applied to ocean acoustics [2]. Numerous subsequent contributions have been made in this area [3]. In this paper, we apply paraxial approximations to 3-D migration problems in geophysics, in which  $z$  is the evolution variable. For this application, Claerbout was the first to introduce 15 and 45° equations for the extrapolation of 2-D seismic data [4,5].

The discretization of the paraxial wave equation involves two kinds of variables, the depth variable  $z$  and the transverse variables  $x_1$  for 2-D problems and  $(x_1, x_2)$  for 3-D problems. One approach for solving paraxial wave equations is based on the use of discrete extrapolation operators [6]. Another approach is based on approximating derivatives with finite differences or finite elements. Paraxial wave equations are commonly used for solving 2-D

---

\* Corresponding author.

*E-mail address:* eliane.becache@inria.fr (E. Bécache).

problems [7]. Their extension to 3-D problems requires the solution at each extrapolation step of a 2-D problem in the transverse plane, which gives rise to a large linear system that can be solved using iterative methods [8,9].

To avoid solving a transverse 2-D problem, Collino and Joly have constructed new families of paraxial approximations that are compatible with splitting methods [1]. In contrast to classical alternating direction methods [10,11], this approach introduces directions for the splitting other than the usual cross-line and in-line directions. This allows one to obtain 45 and 60° approximations that do not contain the undesirable anisotropic effects that arise in Brown's approximation [10]. The problem is then reduced to a series of 2-D extrapolations in each direction. Recently and independently of this work, Ristow and Ruhl used the same idea of operator splitting in alternate directions [12].

In this paper, we describe a systematic way of obtaining accurate discretizations, both in the depth and in the transverse variables, for solving the 3-D paraxial equations introduced in [1] with splitting methods. It is well known that lower order numerical schemes can give rise to numerical dispersion (see [13] for the classical discretization of 2-D paraxial equations). Since dispersion is even more important in 3-D problems, we have developed higher-order numerical schemes that attenuate these effects. We construct our schemes in general heterogeneous media, study their accuracy via a dispersion analysis, and compare them with numerical experiments.

The paper is organized as follows. Section 2 is devoted to the continuous equations. In Section 2.1, we discuss some properties of the classical paraxial approximations. In Section 2.2, we describe the paraxial approximations introduced in [1], which are compatible with four directions of splitting. Section 3 concerns the discretization of a model 2-D equation. Higher-order discretizations in the depth variable are presented in Section 3.2. The discretization in the transverse variable with variational finite differences techniques is presented in Section 3.3. We compare the dispersion of several particular schemes in Section 4. We present numerical experiments in Section 5.

## 2. Multiway splitting for 3-D paraxial equations

### 2.1. The classical paraxial equations

The solution of the wave equation in the whole homogeneous space,

$$\frac{1}{c^2} \frac{\partial^2 v}{\partial t^2} - \frac{\partial^2 v}{\partial x_1^2} - \frac{\partial^2 v}{\partial x_2^2} - \frac{\partial^2 v}{\partial z^2} = 0, \quad (1)$$

with appropriate boundary and initial conditions, can be split into an up-going wave and a down-going wave. We are interested in the up-going wave, which satisfies the one-way wave equation,

$$\frac{d\hat{v}}{dz} + i\frac{\omega}{c} \left(1 - \frac{c^2|k|^2}{\omega^2}\right)^{1/2} \hat{v} = 0, \quad (2)$$

for  $z \geq 0$ , where  $k = (k_1, k_2)$ ,  $|k|^2 = k_1^2 + k_2^2$ , and  $\hat{v}$  is the Fourier transform of  $v$  with respect to both time and the transverse directions,

$$\hat{v}(k_1, k_2, z, \omega) = \int \int \int v(x_1, x_2, z, t) e^{i(k_1 x_1 + k_2 x_2 - \omega t)} dx_1 dx_2 dt. \quad (3)$$

A paraxial equation is an approximation of Eq. (2) that is obtained by replacing the exact square root  $(1 - |k|^2)^{1/2}$  with a rational approximation that we denote by  $(1 - |\kappa|^2)_{\text{ap}}^{1/2}$ , where  $\kappa = (\kappa_1, \kappa_2)$ ,  $\kappa_1 = ck_1/\omega$ , and  $\kappa_2 = ck_2/\omega$ . With this approach, a nonlocal equation is approximated by a partial differential equation.

The rational approximation is designed to be valid when  $c|k|/\omega$  is sufficiently small (i.e., for propagation directions close to the  $z$ -direction). We define the error,

$$e(\kappa) = |(1 - |\kappa|^2)^{1/2} - (1 - |\kappa|^2)_{\text{ap}}^{1/2}|. \quad (4)$$

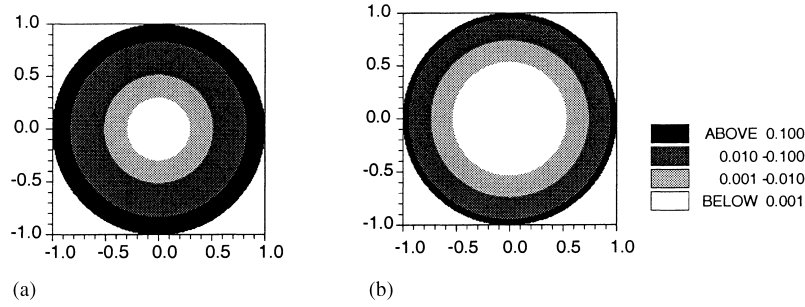


Fig. 1. The error  $e(\kappa)$  of two classical approximations, with respect to  $\kappa_1$  and  $\kappa_2$ . (a)  $15^\circ$  approximation, (b)  $45^\circ$  approximation.

The  $15^\circ$  paraxial equation is based on the linear Taylor expansion,

$$(1 - |\kappa|^2)^{1/2} = 1 - \frac{1}{2}|\kappa|^2 + O(|\kappa|^4). \tag{5}$$

The  $45^\circ$  paraxial equation is based on the Padé approximation,

$$(1 - |\kappa|^2)^{1/2} = \frac{1 - \frac{3}{4}|\kappa|^2}{1 - \frac{1}{4}|\kappa|^2} + O(|\kappa|^6). \tag{6}$$

The accuracy of these two classical approximations is illustrated in Fig. 1, which represents the variations of the error  $e(\kappa_1, \kappa_2)$  with respect to  $\kappa_1$  and  $\kappa_2$  as follows: the larger the white region ( $e(\kappa) \leq 10^{-3}$ ) the better the approximation. Transforming the  $15^\circ$  approximation to physical space and using  $v$  to denote the frequency domain solution, we obtain

$$\frac{\partial v}{\partial z} + \frac{i\omega}{c}v + \frac{ic}{2\omega}\Delta v = 0, \tag{7}$$

where  $\Delta = \partial_1^2 + \partial_2^2$  is the 2-D Laplacian and  $\partial_j \equiv \partial/\partial x_j$ . We handle the second term exactly with the change of variable  $u = ve^{i\omega z/c}$  and obtain the  $15^\circ$  paraxial equation,

$$\frac{\partial u}{\partial z} + \frac{ic}{2\omega}\Delta u = 0. \tag{8}$$

Since  $\Delta$  is a sum of 1-D operators, Eq. (8) can be solved with the splitting method [14], which is useful for solving evolution equations involving a sum of  $N_s$  operators of the form,

$$\frac{\partial u}{\partial z}(\mathbf{x}, z) - i\sum_{j=1}^{N_s} A_j(z)u(\mathbf{x}, z) = 0, \quad z \geq 0, \quad \mathbf{x} = (x_1, x_2) \in \mathbb{R}^2, \quad u(z = 0) = u_0 \text{ in } \mathbb{R}^2. \tag{9}$$

Knowing  $u(z_0)$ , splitting methods involve computing  $u(z_0 + \Delta z)$  in an approximate way. This leads us to define  $N_s$  intermediate unknowns  $w_j$ ,  $j = 1, \dots, N_s$  satisfying

$$\begin{aligned} \frac{\partial w_j}{\partial s}(\mathbf{x}, s) - iA_j(z_0 + s)w_j(\mathbf{x}, s) &= 0, \quad 0 \leq s \leq \Delta z, \quad \mathbf{x} \in \mathbb{R}^2, \\ w_j(s = 0) &= \begin{cases} u(z_0), & \text{for } j = 1, \text{ in } \mathbb{R}^2 \\ w_{j-1}(\Delta z), & \text{for } j > 1, \text{ in } \mathbb{R}^2 \end{cases} \end{aligned} \tag{10}$$

and to set  $u(z_0 + \Delta z) = w_{N_s}(\Delta z)$ . Problem (10) is still an evolution problem in  $z$  but with a single operator.

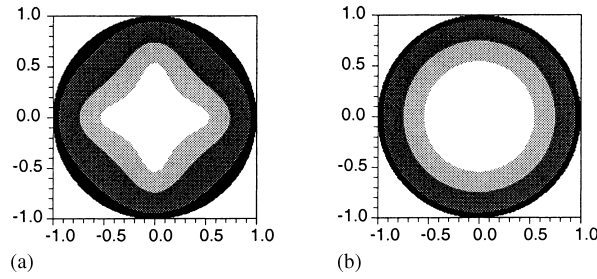


Fig. 2. The error  $e(\kappa)$  of splitting approximations that correspond to (a) two directions (Brown's approximation) and (b) four directions (the Maxi-isotropic approximation,  $b_1 = 0.25$ ).

It is straightforward to apply this technique to Eq. (8) with  $A_j = -c/2\omega\partial_j$  and  $N_s = 2$ . This case involves the solution of 1-D problems in the  $x_1$  and  $x_2$  directions. On the other hand, the splitting method is not efficient when applied directly to the  $45^\circ$  paraxial equation,

$$\frac{\partial u}{\partial z} - iAu = 0, \tag{11}$$

$$A = -\frac{\omega}{2c} \left( \frac{\omega^2}{c^2} + \frac{1}{4}\Delta \right)^{-1} \Delta. \tag{12}$$

Indeed, there is no decomposition of  $A$  into a sum of simple 1-D operators that is consistent with the  $45^\circ$  approximation order. The classical way to approximate Eq. (11), posed in a bounded domain and subject to boundary conditions, is to discretize  $\Delta$  on a uniform grid. This leads to a large, sparse system of equations that can be solved using iterative methods [9]. To avoid this inefficient approach, Brown [10] has suggested the approximation,

$$(1 - |\kappa^2|)^{1/2} = 1 - \frac{\frac{1}{2}\kappa_1^2}{1 - \frac{1}{4}\kappa_1^2} - \frac{\frac{1}{2}\kappa_2^2}{1 - \frac{1}{4}\kappa_2^2} + O(\kappa_1^2\kappa_2^2), \tag{13}$$

which has been used by other authors [11]. The accuracy of this approximation is highly anisotropic. The error is consistent with the  $45^\circ$  equation ( $e(\kappa) = O(|\kappa|^6)$ ) in the  $\kappa_1 = 0$  and  $\kappa_2 = 0$  directions. In other directions, the approximation is only slightly better than the  $15^\circ$  approximation, as one can see by comparing Figs. 1 and 2.

2.2. *The four-way splitting equations*

The basic idea developed in [1] is to achieve greater accuracy for approximations involving only one transverse space variable per fraction by introducing more than two directions of splitting. The simplest family of paraxial equations is based on the four directions of splitting,  $x_1, x_1 + x_2, x_1 - x_2, x_2$ , and the rational approximation,

$$(1 - |\kappa^2|)^{1/2} \cong 1 - R(\kappa), \tag{14}$$

$$R(\kappa) = \sum_{j=1}^4 \frac{b_j(\kappa \cdot n_j)^2}{1 - a_j(\kappa \cdot n_j)^2}, \tag{15}$$

where  $n_j = (\cos \alpha_j, \sin \alpha_j)$  is the unit vector associated with the  $j$ th direction  $\alpha_j = (j - 1)\pi/2$ . The conditions  $a_j > 0$  and  $b_j \geq 0$  must be satisfied to ensure well-posedness. To prevent the approximation error in the square root from blowing-up in certain directions inside the unit disk  $|\kappa| \leq 1$ , it is necessary to require  $0 < a_j \leq 1$ . Approximations consistent with the  $45^\circ$  approximation (i.e., such that  $e(\kappa) = O(|\kappa|^6)$ ) correspond to a system

satisfied by the coefficients  $a_j$  and  $b_j$ . This leads to a family of  $45^\circ$  approximations depending on one parameter  $b_1$  that has to be chosen in the interval  $[1/12, 5/12]$  in order to ensure the conditions  $0 < a_j \leq 1$  and  $b_j \geq 0$ :

$$b_4 = b_1, \quad b_2 = b_3 = \frac{1 - 2b_1}{2}, \quad a_1 = a_4 = \frac{1}{12b_1}, \quad a_2 = a_3 = \frac{1}{12b_2}. \tag{16}$$

Criteria based on the error  $e(\kappa)$  are proposed for the choice of  $b_1$  in [1]. In Fig. 2, we present the error of the so-called maxi-isotropic  $45^\circ$  approximation, which corresponds to  $b_1 = \frac{1}{4}$ . In contrast to Brown’s approximation, the quality of this approximation is comparable to the classical  $45^\circ$  approximation not only in the  $\kappa_1$  and  $\kappa_2$  directions but also in all other directions. The paraxial equation corresponding to Eq. (14) is

$$\frac{\partial u}{\partial z} - i \frac{\omega}{c} \sum_{j=1}^4 A_j u = 0, \tag{17}$$

$$A_j = -b_j \left( \frac{\omega^2}{c^2} + a_j D_j^2 \right)^{-1} D_j^2, \tag{18}$$

where  $D_j = n_j \cdot (\partial_1, \partial_2)$  is the directional derivative. Since each  $A_j$  is a 1-D operator, this family of equations lends itself to a splitting method in the horizontal variables.

It was shown in [1] how to design other families of paraxial approximations of a given order of accuracy, introducing either more than four directions for the splitting or more than one fraction per direction. We consider approximations based on four splitting directions, which are relatively easy to implement on regular grids. This is not a significant restriction because four directions are sufficient to achieve accurate solutions (e.g.,  $60^\circ$  approximations) by increasing the number of fractions per direction.

Paraxial equations in heterogeneous media were proposed and analyzed in [15]. These equations are based on defining several criteria, both mathematical and physical in nature, and selecting from a general class of possible candidates the one that satisfies these criteria. This approach can be used to extend any paraxial equation to heterogeneous media. Using this approach to generalize Eqs. (17) and (18), we define the new variable  $\tilde{u} = u/c^{1/2}$  and obtain

$$A_j = -b_j (\omega^2 + a_j \Delta_j^c)^{-1} \Delta_j^c, \tag{19}$$

where  $\Delta_j^c = (cD_j)^2$  and  $c$  depends on  $(x_1, x_2, z)$ . Paraxial equations have also been developed for problems involving variations in density and other parameters [16,17].

For the numerical computation, the problem is defined in the cylindrical domain  $\mathcal{D} \times \{z \geq 0\}$ . When  $\mathcal{D}$  is unbounded, it is necessary to introduce artificial transverse boundaries, designed such that the waves are absorbed when they reach the boundaries. The concept of a perfectly matched layer (PML), which was originally introduced for Maxwell’s equations [18], has been adapted to paraxial equations [19]. This approach is based on replacing  $\Delta_j^c$  with

$$\tilde{\Delta}_j^c = (cd_j(x_1, x_2)D_j)^2, \tag{20}$$

$$d_j(x_1, x_2) = \frac{i\omega}{i\omega + c\sigma_j(x_1, x_2)}, \tag{21}$$

where the damping  $\sigma_j > 0$  has support in a damped region that surrounds the region of interest in the  $(x_1, x_2)$  plane and is only a function of the space coordinate corresponding to directions parallel to vector  $n_j$ . An approach for constructing  $\sigma_j$  is given in [20]. It can be shown by a plane wave analysis that the PML model possesses the remarkable property of generating no reflection at the interface between the region of interest and the artificial lossy medium. Furthermore, waves are exponentially damped in the absorbing layer.

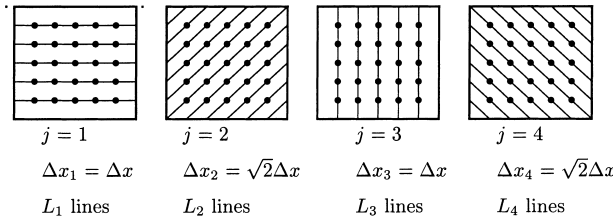


Fig. 3. Computational grid for the  $45^\circ$  approximation with four directions of splitting.

### 3. Higher-order schemes for the four-way splitting equations

The approximation of the 3-D paraxial equation involves three steps. We first reduce the problem to a series of 2-D paraxial equations using splitting techniques so that it is sufficient to know how to discretize a 2-D model equation. In the second step, we discretize with finite differences in  $z$ . In the third step, we discretize along the transverse variable with variational finite differences.

#### 3.1. Reduction to a series of 2-D paraxial equations

Applying the splitting technique to the 3-D paraxial Eq. (17) with Dirichlet boundary conditions, we obtain a series of 2-D paraxial equations. More precisely, the knowledge of  $u(z_0 + \Delta z)$  from  $u(z_0)$  consists in solving  $N_D = 4$  problems as in Eq. (10). In a heterogeneous medium, it can be rewritten using the auxiliary unknowns  $\varphi_j(\mathbf{x}, s) = A_j(\mathbf{x}, z_0 + s)w_j(\mathbf{x}, s)$ ,  $1 \leq j \leq N_D$  as

$$\begin{aligned} \frac{\partial w_j}{\partial s}(\mathbf{x}, s) - i\frac{\omega}{c}\varphi_j(\mathbf{x}, s) &= 0, \quad \mathbf{x} = (x_1, x_2) \in \mathcal{D}, \quad 0 \leq s \leq \Delta z, \\ \frac{\omega^2}{c}\varphi_j + D_j(cD_j(a_j\varphi_j + b_jw_j)) &= 0, \quad (\mathbf{x}, s) \in \mathcal{D} \times [0, \Delta z], \\ w_j(s=0) &= \begin{cases} u(z_0) & \text{for } j=1, \\ w_{j-1}(\Delta z) & \text{for } 2 \leq j \leq N_D \end{cases} \end{aligned} \quad (22)$$

and we obtain  $u(z_0 + \Delta z) = w_{N_D}(\Delta z)$ . We let  $\mathcal{G}^j$  be a grid composed on lines parallel to direction  $j$  as show in Fig. 3. The problem defined in Eq. (22) can be decomposed as several problems, posed on each line independently. On one particular line  $\Omega$ , the problem can be written as Eq. (22), with the exception that  $x$  varies only on  $\Omega$ . This equation is simply a 2-D paraxial equation.

Without loss of generality, we focus on a particular direction  $x$ , take  $\Omega = (-L, L)$ , and solve the 2-D paraxial equation,

$$\begin{aligned} \frac{\partial w}{\partial z} - \frac{i\omega}{c}\varphi &= 0 && \text{in } \Omega \times [0, Z], \\ \frac{\omega^2}{c}\varphi + \frac{\partial}{\partial x} \left( c \frac{\partial}{\partial x} (a\varphi + bw) \right) &= 0 && \text{in } \Omega \times [0, Z], \\ w(z=0) &= w_0 && \text{in } \Omega, \\ w \equiv \varphi &\equiv 0 && \text{on } \partial\Omega \times [0, Z], \end{aligned} \quad (23)$$

where  $a > 0$  and  $b \geq 0$  and  $w$  is related to the 2-D wave field  $v$  via the change of unknown  $w = e^{i(\omega/c)z}v$ . To obtain a variational formulation of Eq. (23), we introduce the notations,

$$\begin{aligned}
 (u, v)_{0,\Omega} &= \int_{\Omega} u\bar{v} \, dx, \quad \|u\|_{0,\Omega} = (u, u)_{0,\Omega}^{1/2}, \quad |\phi|_{1,\Omega} = \left( \int_{\Omega} \left| \frac{\partial \phi}{\partial x} \right|^2 \, dx \right)^{1/2}, \\
 H &= L^2(\Omega) = \left\{ u, \int_{\Omega} |u|^2 \, dx < \infty \right\}, \quad V = H_0^1(\Omega) = \left\{ u \in H, \frac{du}{dx} \in H, u = 0 \text{ on } \partial\Omega \right\}, \\
 m(u, v) &= \int_{\Omega} \frac{1}{c} u\bar{v} \, dx, \quad \forall (u, v) \in H, \quad k(u, v) = \int_{\Omega} c \frac{\partial u}{\partial x} \frac{\partial \bar{v}}{\partial x} \, dx, \quad \forall (u, v) \in V,
 \end{aligned} \tag{24}$$

where  $m(\cdot, \cdot)$  and  $k(\cdot, \cdot)$  are the mass and stiffness bilinear forms. Let  $w_0$  be in  $V$ . The variational formulation of Eq. (23) consists in finding  $(w, \varphi) : [0, Z] \rightarrow V \times V$  such that

$$\begin{aligned}
 \frac{d}{dz}(w, \chi) - i\omega m(\varphi, \chi) &= 0 \quad \forall \chi \in V, \\
 \omega^2 m(\varphi, \chi) - k(a\varphi + bw, \chi) &= 0 \quad \forall \chi \in V, \\
 w(z = 0) &= w_0.
 \end{aligned} \tag{25}$$

We recall the classical  $L^2$ -stability result that any solution  $(w, \varphi)$  to Eq. (25) satisfies the energy conservation condition,  $\|w(z)\|_{0,\Omega} = \|w_0\|_{0,\Omega}, \forall z$  [8].

### 3.2. Semi-discretization in depth

We assume that  $c(x_1, x_2, z) = c^m(x_1, x_2)$  for  $z \in [z^m, z^{m+1}]$ . In each interval  $[z^m, z^{m+1}]$ , Eq. (23) is rewritten as

$$\frac{dw}{dz} = iC^m w, \quad z^m \leq z \leq z^{m+1}, \quad w(z^m) = w^m, \tag{26}$$

where  $C^m = -\omega/c^m(\omega^2 + a\Delta_m^c)^{-1}b\Delta_m^c$  and  $\Delta_m^c = c^m\partial/\partial x(c^m\partial/\partial x)$ . In order to obtain conservative schemes, we use the discretization in depth proposed in [8]. This approach is based on the expression of the exact solution of (26),  $w(z^{m+1}) = e^{iC^m\Delta z}w(z^m)$  and the Padé approximant of the exponential,

$$\prod_{k=1}^K \frac{1 + r_k x}{1 + \bar{r}_k x} = \frac{N_K(x)}{N_K(x)} \text{ with } r_k \text{ such that } e^{ix} = \frac{N_K(x)}{N_K(x)} + O(|x|^{2K}), \tag{27}$$

where  $N_K(x) = \prod_{k=1}^K (1 + r_k x)$ . The integration from  $z^m$  to  $z^{m+1}$  is then formally done as follows:  $w^{m+1} = \prod_{k=1}^K (I + \bar{r}_k \Delta z C^m)^{-1} (I + r_k \Delta z C^m) w^m$ . This procedure leads us to define  $K + 1$  intermediate unknowns

$$w_0^m = w^m, \quad (I + \bar{r}_k \Delta z C^m) w_k^m = (I + r_k \Delta z C^m) w_{k-1}^m, \quad 1 \leq k \leq K. \tag{28}$$

We then set  $w^{m+1} = w_K^m$ . The Crank–Nicolson second-order scheme is obtained for the case  $K = 1$  and  $r_1 = i/2$ .

### 3.3. Discretization in the transverse variable with higher-order variational finite difference schemes

The discretization in  $x$  of Eq. (23) is based on the variational formulation (25), which provides a systematic treatment of heterogeneous media and insures stability based on energy estimates. The usual approach is to apply standard Galerkin finite elements  $P_k$  [21], but this would yield several drawbacks, especially in view of the use of the splitting method to get the 3-D solution, see [20]. One difficulty is related to the fact that, for higher-order  $P_k$  finite elements ( $k \geq 2$ ), there are additional degrees of freedom between two mesh points. Since these new degrees of freedom do not coincide in each direction of splitting, the evaluation of the solution at these points would require the use of interpolation procedures. Another difficulty is related to the approach for introducing the so-called modified schemes, which are essentially based on the use of an approximate mass matrix. With a finite element approach,

this could still be done using a mass-lumping technique, but this is not always possible with the classical degrees of freedom [22]. We prefer to use a variational finite difference approach. The proofs are omitted but can be found in [20].

### 3.3.1. Presentation of the discretization

We discretize the domain with a regular grid  $x_i = ih$  and define the shifted grid by the nodes  $x_{i+1/2} = (i + 1/2)h$ . We look for an approximate solution of Eq. (25),  $(w_h, \varphi_h) : [0, Z] \rightarrow (H_h)^2$ , where

$$H_h = \{v_h \in L^2(\Omega); v_h|_{[x_{i-1/2}, x_{i+1/2}]} \in P^0, v_h(x_0) = v_h(x_{N+1}) = 0\}, \quad (29)$$

is a finite dimensional space which is only included in  $L^2(\Omega)$  and not in  $V$  ( $P^0$  is the space of constant functions). Therefore,  $k(\cdot, \cdot)$  needs to be approximated by a bilinear form  $k_h(\cdot, \cdot)$  defined on  $H_h$  (see below), and we have to solve

$$\begin{aligned} \frac{d}{dz}(w_h, \chi_h) - i\omega m(\varphi_h, \chi_h) &= 0 \quad \forall \chi_h \in H_h, \\ \omega^2 m(\varphi_h, \chi_h) - k_h(a\varphi_h + bw_h, \chi_h) &= 0 \quad \forall \chi_h \in H_h. \end{aligned} \quad (30)$$

Let  $(\chi_i)_{i=1, \dots, N}$  be the basis of  $H_h$  defined such that  $\chi_i(x_j) = \delta_{ij}/\sqrt{h}$  for  $1 \leq i, j \leq N$  and  $(\chi_i, \chi_j)_0 = \delta_{ij}$ . The approximate solution is decomposed as  $w_h(x, z) = \sum_{i=1}^N W_i(z)\chi_i(x)$ ,  $\varphi_h(x, z) = \sum_{i=1}^N \Phi_i(z)\chi_i(x)$  and Eq. (30) is equivalent to find the vector functions  $(W_h, \Phi_h)$  satisfying

$$\frac{dW_h}{dz} - i\omega M_h \Phi_h = 0, \quad (\omega^2 M_h - aK_h)\Phi_h = bK_h W_h, \quad (31)$$

where  $M_h$  is a diagonal definite positive matrix, called the mass matrix,  $(M_h)_{ij} = m(\chi_i, \chi_j)$ ,  $K_h$  is the stiffness matrix,  $(K_h)_{ij} = k_h(\chi_i, \chi_j)$ , and  $k_h$  will be defined below.

### 3.3.2. Definition of the approximate stiffness bilinear form $k_h$

To derive an approximate stiffness bilinear form, the derivative  $\partial/\partial x$  is approximated with a finite difference operator defined on  $H_h$ . Let  $D_\varepsilon$  denote the usual second-order finite difference  $D_\varepsilon \phi(x) \equiv \phi(x + \varepsilon) - \phi(x - \varepsilon)$ , and  $D_\varepsilon^*$  its adjoint, defined as  $D_\varepsilon^* = -D_\varepsilon$ . For  $\phi \in H_h$ , and  $\varepsilon = h/2$ , we define  $D_{h/2}\phi(x) = \phi(x_i) - \phi(x_{i-1})$ , for  $x \in [x_{i-1}, x_i]$ , so that

$$D_{h/2}\phi \in H_h^{1/2} = \{v_h \in L^2(\Omega) \text{ such that } v_h|_{[x_{i-1}, x_i]} \in P^0, \quad \forall 1 \leq i \leq N + 1\}.$$

More generally, if we consider the finite difference operator  $D_{(2p-1)h/2}$ , we have  $D_{(2p-1)h/2}\phi \in H_h^{1/2}$ , where  $\phi$  is extended to zero outside  $\Omega$ . We introduce some real numbers  $v_p$  and set

$$\partial_h = \frac{1}{h} \sum_{p=1}^n v_p D_{(2p-1)h/2}. \quad (32)$$

In particular we have  $\partial_h \phi(x_{j+1/2}) = \sum_{p=1}^n v_p (\phi(x_{j+p}) - \phi(x_{j-p+1}))/h$ , and if  $\phi \in H_h$ , then  $\partial_h \phi$  is in  $H_h^{1/2}$ . We have the following lemma [20].

**Lemma 3.1.** *The approximation (32) is of order  $2n$  – i.e., for any regular  $\rho$ ,  $\partial_h \rho(x) = d\rho(x)/dx + O(h^{2n})$ ,  $\forall x$  – provided that coefficients  $v_p$  satisfy*

$$\sum_{p=1}^n v_p (2p-1)^{2k-1} = \delta_{k1} \quad \text{for } 1 \leq k \leq n. \quad (33)$$

*In that case it is denoted by  $\partial_h^{[2n]}$  and for any regular function  $\rho$  we have*

$$\begin{aligned} \partial_h^{[2n]} \rho(x) &= \frac{d\rho}{dx}(x) + h^{2n} R_S^{[2n]} \rho^{(2n+1)}(x) + O(h^{2n+2}), \\ R_S^{[2n]} &= \frac{\sum_{p=1}^n \nu_p (2p-1)^{2n+1}}{(2n+1)! 2^{2n}}. \end{aligned} \tag{34}$$

System (33) has a unique solution given explicitly in Eqs. (45) and (47). We now define the approximate stiffness bilinear form and stiffness matrix,

$$\begin{aligned} k_h^{[2n]}(\phi, \chi) &= (c \partial_h^{[2n]} \phi, \partial_h^{[2n]} \chi) \quad \forall (\phi, \chi) \in H_h^2, \\ (K_h)_{ij}^{[2n]} &= k_h^{[2n]}(\chi_i, \chi_j). \end{aligned} \tag{35}$$

3.3.3. The classical schemes

With the above definitions, we define the second-order classical scheme as

$$\frac{dW_h}{dz} - i\omega M_h \Phi_h = 0, \tag{36}$$

$$(\omega^2 M_h - a K_h^{[2n]}) \Phi_h = b K_h^{[2n]} W_h. \tag{37}$$

After elimination of the auxiliary unknown, we get the evolution system

$$(\omega^2 M_h - a K_h^{[2n]}) M_h^{-1} \frac{dW_h}{dz} = i\omega b K_h^{[2n]} W_h. \tag{38}$$

This requires the inversion of  $M_h$ , which is easy since  $M_h$  is diagonal. This property is important to keep in mind when constructing the new modified schemes.

We now analyze the order of the scheme in a homogeneous medium. Eq. (36) can then be rewritten in the form, for all  $j$ ,

$$\frac{dw_h}{dz}(x_j, z) - \frac{i\omega}{c} \varphi_h(x_j, z) = 0, \quad \frac{\omega^2}{c} \varphi_h(x_j, z) - \sum_i (K_h^{[2n]})_{ji} (a\varphi_h(x_i, z) + bw_h(x_i, z)) = 0. \tag{39}$$

To analyze this approximation, we choose as a criterion of quality the truncation error that quantifies the order at which the exact solution  $(w, \varphi)$  of Eq. (23) satisfies the scheme. The first equation is obviously satisfied by the exact solution. The error therefore comes from the second equation,

$$E_h^{\text{class}} = \frac{\omega^2}{c} \varphi(x_j, z) - \sum_i (K_h^{[2n]})_{ji} (a\varphi(x_i, z) + bw(x_i, z)). \tag{40}$$

**Lemma 3.2.** *The scheme (36) is of order  $2n$ . The first term of the truncation error is of the form,*

$$E_h^{\text{class}} = 2c R_S^{[2n]} h^{2n} \frac{\partial^{2n+2}(a\varphi + bw)}{\partial x^{2n+2}}(x_j, z) + O(h^{2n+2}), \tag{41}$$

where  $R_S^{[2n]}$  defined in Eq. (34).

3.3.4. The modified schemes

The idea of the modified schemes is to approximate  $M_h$  in the first term of Eq. (38) with a matrix  $M_{h,\alpha}^{[2n]}$  that provides improved accuracy while preserving the bandwidth of the system to maintain the same computational cost. This corresponds to modifying the mass matrix only in Eq. (37) to obtain

$$\frac{dW_h}{dz} - i\omega M_h \Phi_h = 0, \quad (\omega^2 M_{h,\alpha}^{[2n]} - a K_h^{[2n]}) \Phi_h = b K_h^{[2n]} W_h. \tag{42}$$

The mass matrix is defined as  $(M_h)_{ij} = (1/c\chi_i, \chi_j)_0$ . We introduce the approximation,  $I_\varepsilon\phi(x) = (\phi(x + \varepsilon) + \phi(x - \varepsilon))/2(I_\varepsilon^* = I_\varepsilon)$  of the identity operator  $I$ . For  $\phi \in H_h$  and  $\varepsilon = (2p - 1)h/2$ , we obtain  $I_\varepsilon\phi \in H_h^{1/2}$ . We define

$$\mathcal{I}_h = \sum_{p=1}^n \mu_p I_{(2p-1)h/2}, \text{ where } \mu_p \text{ are real numbers.} \tag{43}$$

**Lemma 3.3.** *The approximation (43) is of order  $2n$  - i.e.,  $\mathcal{I}_h\rho(x) = \rho(x) + O(h^{2n})$ ,  $\forall x$ , for any regular function  $\rho$  - if coefficients  $\mu_p$  are the unique solutions of the Vandermonde system*

$$\sum_{p=1}^n \mu_p (2p - 1)^{2(k-1)} = \delta_{k1} \quad \text{for } 1 \leq k \leq n, \tag{44}$$

given by

$$\mu_p = \frac{\prod_{m \neq p} (2m - 1)^2}{\prod_{m \neq p} ((2m - 1)^2 - (2p - 1)^2)}. \tag{45}$$

In this case, it is denoted  $\mathcal{I}_h^{[2n]}$  and for any regular function  $\rho$  we have

$$\begin{aligned} \mathcal{I}_h^{[2n]}\rho(x) &= \rho(x) + h^{2n} R_M^{[2n]}\rho^{(2n)}(x) + O(h^{2n+2}), \\ R_M^{[2n]} &= \frac{\sum_{p=1}^n \mu_p (2p-1)^{2n}}{(2n)!2^{2n}}. \end{aligned} \tag{46}$$

**Lemma 3.4.** *The coefficients  $v_p$  and  $\mu_p$  satisfy the relation*

$$\mu_p = (2p - 1)v_p, \quad 1 \leq p \leq n. \tag{47}$$

We can now construct an approximate symmetric and positive mass matrix

$$(\mathcal{M}_h^{[2n]})_{ij} = \left( \frac{1}{c} \mathcal{I}_h^{[2n]}\chi_i, \mathcal{I}_h^{[2n]}\chi_j \right)_0. \tag{48}$$

**Remark 3.1.** *For the same value of  $n$ , the approximations  $\mathcal{I}_h^{[2n]}\chi_i$  and  $\partial_h^{[2n]}\chi_i$  use the values of the function at the same points. The matrices  $\mathcal{M}_h^{[2n]}$  and  $K_h^{[2n]}$  therefore have the same bandwidth.*

The idea is now to introduce the convex combination of both mass matrices (which remains positive definite and thus invertible),

$$M_{h,\alpha}^{[2n]} = \alpha M_h + (1 - \alpha)\mathcal{M}_h^{[2n]}, \quad 0 \leq \alpha \leq 1, \tag{49}$$

and to look for a particular value of  $\alpha$  in order to gain accuracy relative to the classical discretization, which corresponds to  $\alpha = 1$ . From Remark 3.1, we see that  $\omega^2 M_{h,\alpha}^{[2n]} - aK_h^{[2n]}$  has the same bandwidth as the classical scheme. To analyze the order of this scheme, we write it in a homogeneous medium as

$$\frac{dw_h}{dz}(x_j, z) - \frac{i\omega}{c}\varphi_h(x_j, z) = 0, \quad \omega^2 \sum_i (M_{h,\alpha}^{[2n]})_{ji}\varphi_h(x_i, z) - \sum_i (K_h^{[2n]})_{ji}(a\varphi_h + bw_h)(x_i, z) = 0, \tag{50}$$

and the truncation error still comes from the second equation

$$E_h^{\text{mod}} = \omega^2 \sum_i (M_{h,\alpha}^{[2n]})_{ji}\varphi(x_i, z) - \sum_i (K_h^{[2n]})_{ji}(a\varphi + bw)(x_i, z), \tag{51}$$

where  $(w, \varphi)$  is the exact solution of Eq. (23), assumed regular enough.

**Proposition 3.1.** *The modified scheme (42), with the matrix  $M_{h,\alpha}^{[2n]}$  defined in (49) is of order  $2n+2$  in a homogeneous medium with the choice*

$$\alpha = \alpha^{[2n]} = \frac{2n}{2n+1}. \tag{52}$$

We can easily relate modified schemes to Claerbout’s scheme. Actually, the classical Claerbout’s scheme [5] is usually seen as a modification of the stiffness matrix in Eq. (31). The second-order approximation  $K_h^{[2]}$  is replaced by  $(I - \gamma h^2 K_h^{[2]})^{-1} K_h^{[2]}$  which is still of second-order and becomes fourth-order with the value  $\gamma = 1/12$ . In the modified schemes, the modification plays on the mass matrix, but it can also be interpreted as a modification on the stiffness matrix by rewriting the modified mass matrix as  $M_{h,\alpha}^{[2n]} = (I + (1 - \alpha)(\mathcal{M}_h^{[2n]} - M_h)M_h^{-1})M_h$ , and multiplying the second equation by  $(I + (1 - \alpha)(\mathcal{M}_h^{[2n]} - M_h)M_h^{-1})^{-1}$  in order to reobtain  $M_h$  for the mass term. The stiffness matrix is then modified and becomes

$$A_{h,\alpha}^{[2n]} = (I + (1 - \alpha)(\mathcal{M}_h^{[2n]} - M_h)M_h^{-1})^{-1} K_h^{[2n]}. \tag{53}$$

The modified scheme can then be rewritten as follows:

$$\frac{dW_h}{dz} - i\omega M_h \Phi_h = 0, \quad \omega^2 M_h \Phi_h - A_{h,\alpha}^{[2n]}(a\Phi_h + bW_h) = 0. \tag{54}$$

For  $n = 1$ , the fourth-order modified scheme is equivalent to Claerbout’s scheme with the relation  $\gamma = (1 - \alpha)/4$ . The higher-order modified schemes can thus be interpreted as an extension to higher-orders of Claerbout’s scheme.

3.3.5. *Stability analysis*

It is convenient to analyze the well-posedness of the schemes written in the form in Eq. (54) (rather than Eq. (42)), which is very close to the continuous equations.

**Proposition 3.2.** *If the matrix  $A_{h,\alpha}^{[2n]}$  defined in Eq. (53) satisfies the condition*

$$A_{h,\alpha}^{[2n]} V_h \cdot V_h \in \mathbb{R} \quad \forall V_h, \tag{55}$$

*then the approximate problem (54) has a unique solution  $(W_h, \Phi_h)$  that satisfies the energy conservation:  $\|W_h(z)\| = \|W_h(0)\|, \quad \forall z$ . The classical schemes ( $\alpha = 1$ ) satisfy condition (55), for any medium. The modified schemes satisfy (55) in a homogeneous medium.*

There is a technical difficulty for proving the stability of the modified schemes in heterogeneous media [20]. However, numerical experiments show that the modified schemes are stable, even in heterogeneous media.

3.4. *Algorithm*

Let  $U_h^m$  be the approximate solution of the 3-D Eq. (17), at step  $z_m$ . The algorithm to compute the solution  $U_h^{m+1}$  is summarized as follows. Introduce  $N_D + 1$  intermediate unknowns,  $(W^{m,j})_{j=0,\dots,N_D}$ , where  $W^{m,0} = U_h^m$  is the initialization (here  $N_D = 4$ ). For each direction  $1 \leq j \leq N_D$ , on each mesh-line in this direction,  $1 \leq l_j \leq L_j$  (see Fig. 3),  $W^{m,j}$  is determined as  $W^{m,j} = W_j^m(\Delta z)$  where  $W_j^m$  is the solution of the 2D paraxial equation on this line

$$\frac{dW_j^m}{ds} = iC_h^{j,m} W_j^m, \quad 0 \leq s \leq \Delta z, \quad W_j^m(0) = W^{m,j-1}, \tag{56}$$

with  $C_h^{j,m} = \omega M_h (\omega^2 M_\alpha^{[2n]} - a_j K_h^{[2n]})^{-1} b_j K_h^{[2n]}$  (with the modified schemes). The matrices depend on  $m$ , on  $j$  and on the line  $l_j$ . In particular, in a diagonal direction, the size of the matrices is different on each line. Note that the step-size also depends on the direction. To solve Eq. (56), we follow Section 3.2: introduce  $K + 1$  intermediary

unknown vectors  $(\tilde{W}_j^m)_{k,k=0,\dots,K}$ , where  $(\tilde{W}_j^m)_0 = W^{m,j-1}$  and for  $k = 1, \dots, K$ ,  $(\tilde{W}_j^m)_k$  is solution of the linear system

$$S_k^{m,j} (\tilde{W}_j^m)_k = \bar{S}_k^{m,j} (\tilde{W}_j^m)_{k-1} \tag{57}$$

with  $S_k^{m,j} = (\omega^2 a_j M_\alpha^{[2n]} - K_h^{[2n]})(M_h)^{-1} + \bar{r}_k \omega \Delta z b_j a_j K_h^{[2n]}$ . The last step gives us  $W^{m,j} \equiv (\tilde{W}_j^m)_K$ . Finally the solution at  $z^{m+1}$  is given by  $U_h^{m+1} = W^{m,N_D}$ .

**4. Dispersion analysis**

We only consider the modified schemes of order  $2n+2$  obtained with the particular choice of  $\alpha = \alpha^{[2n]}$ . A scheme obtained using a classical  $2n$  order discretization in  $x$  and a  $2K$  order discretization in  $z$  will be called  $2nx_{\text{class}} - 2Kz$  scheme. A scheme obtained using a modified  $2n$  order discretization in  $x$  and a  $2K$  order discretization in  $z$  will be called  $2nx_{\text{mod}} - 2Kz$  scheme.

The dispersion analysis consists in analyzing the propagation of plane waves in a homogeneous medium,  $v(x, z) = \exp\{-i(k_x x + k_z z)\}$  with  $k = (k_x, k_z)$ . For the harmonic wave equation, the dispersion relation is  $k_x^2 + k_z^2 = \omega^2/c^2$ , which is equivalent to  $(p_e^{\text{wave}})^2 = p_a^2/(1 - p_a^2)$ , if we set  $p_a = ck_x/\omega = \tan \theta_a$  and  $p_e = k_x/k_z = \tan \theta_e$ . The dispersion relation for the  $45^\circ$  paraxial equation is  $(ck_z/\omega)^{\text{cont}} = 1 - bp_a^2/(1 - ap_a^2) = p_a/p_e^{\text{cont}}$ .

We make a similar plane wave analysis for the schemes by looking for solutions on the form  $v_j^m = \exp\{-i(k_x j \Delta x + k_z m \Delta z)\}$ , but this time  $p_e^{\text{num}}$ , not only depends on  $p_a$  but also on  $\omega$ ; this is the numerical dispersion. The weaker this dependence, the better the scheme. To evaluate the quality of the scheme, we define the dispersion error  $E = |\theta_e^{\text{cont}} - \theta_e^{\text{num}}|$ . This quantity depends on the ratio  $r_{zx} = \Delta z/\Delta x$  and the number  $G = 2\pi c/(\omega \Delta x)$  of discretization points per wavelength in  $x$ , the propagation angle  $p_a < 1$ , and the coefficients  $a$  and  $b$  of the paraxial approximation. The dispersion error permits us to make comparisons between several schemes. We restrict the analysis to  $a = 1/4, b = 1/2, p_a = \tan(32^\circ)$  and  $r_{zx} = 1$  (otherwise mentioned), so that  $E$  becomes only a function of  $H = 1/G$ . We have compared the  $(2nx - 2Kz)$  classical and modified schemes for  $K = 1, 2$  and  $n = 1, 2, 3$  and we give some conclusions of these comparisons (see [20] for more details). The comparison between modified and classical schemes shows that, for a given order of accuracy, the less expensive modified schemes have the unexpected property to be always less dispersive than the classical ones. We illustrate this in Fig. 4(a) for the fourth-order schemes in  $x$  and second-order in  $z$ . Since higher-order schemes are more expensive, one can ask if, to achieve greater accuracy, it would be better to refine the mesh. Fig. 4(b) shows that even if we divide the step size by 4, the second-order  $z$ -discretization is more dispersive than the fourth-order one, so that it is better to increase the order of the scheme than to refine the mesh. The last comparison between schemes  $4x_{\text{mod}} - 4z$  and  $6x_{\text{mod}} - 2z$ , in Fig. 4(c), shows that, although the  $z$  and  $x$  directions play different roles in the equations, it is better to take the same order for both discretizations, at least for sufficiently fine meshes (more than 2.5 points per wavelength).

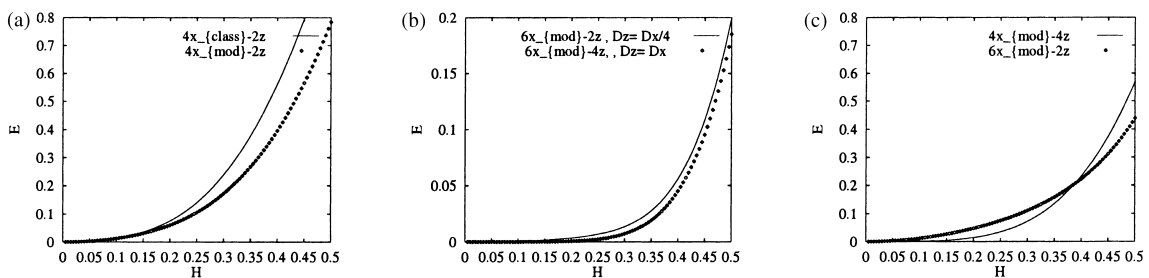


Fig. 4. Behavior of the dispersion error with respect to the inverse of number of points per wavelength: (a) Modified and Classical schemes (fourth-order in  $x$  and second-order in  $z$ ); (b)  $6x_{\text{mod}} - 2z$  with  $r_{zx} = 1/4$  and  $6x_{\text{mod}} - 4z$  with  $r_{zx} = 1$ ; (c)  $4x_{\text{mod}} - 4z$  and  $6x_{\text{mod}} - 2z$ .

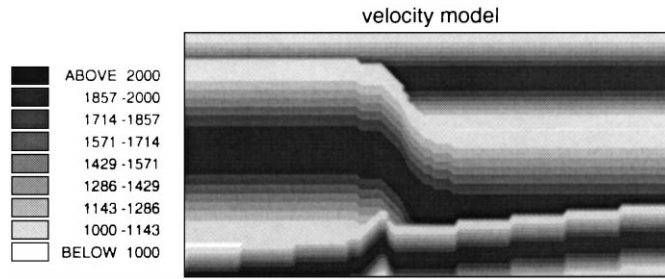


Fig. 5. 2-D smooth heterogeneous medium: level lines of the velocity.

### 5. Numerical experiments

We illustrate the method by several experiments in the time domain, for which we specify the surface data  $v_0(x, t)$ , solve the problem for each frequency, recover the transient result through a Fourier transform, and indicate the cutoff frequency  $F_c$ . The computational domain is 1250 m long in each horizontal direction and 625 m in the vertical direction. The grid sizes are  $h = \Delta z = 12.5$  m. We handle 120 equidistributed frequencies. We represent the solution at time  $T_{\text{obs}}$ , when the wave reaches 80% of the total depth (i.e., 500 m). For each of the experiments, the use of higher-order schemes provides satisfactory results even for a small number of discretization points per wavelength.

#### 5.1. Filtered point source in a 2-D heterogeneous medium

The initial condition at  $z = 0$  is a filtered point source ( $\mathcal{F}_{x,t}$  is the  $(x, t)$  Fourier transform)

$$v_0(x, t) = \frac{d^2}{dt^2}(g_{\omega_S}(t))\delta(x - x_S) * \mathcal{F}_{x,t}^{-1}(1_{|ck_x| < |\omega|}) \equiv \frac{d^2}{dt^2}(g_{\omega_S}(t)) * \mathcal{F}_t^{-1}\left(\frac{2 \sin(\omega|x - x_S|/c)}{|x - x_S|}\right),$$

where  $g_{\omega_S}(t) = \exp(-\omega_S^2 t^2/4)$ . The filtering process eliminates the evanescent modes present in the wave equation. The simulation is performed in the smoothly varying velocity medium shown in Fig. 5. The central frequency of the source is  $F_S = 2\pi c/\omega_S = 28$  Hz and the cutoff frequency is  $F_C = 76$  Hz. The mesh contains about 3 points per

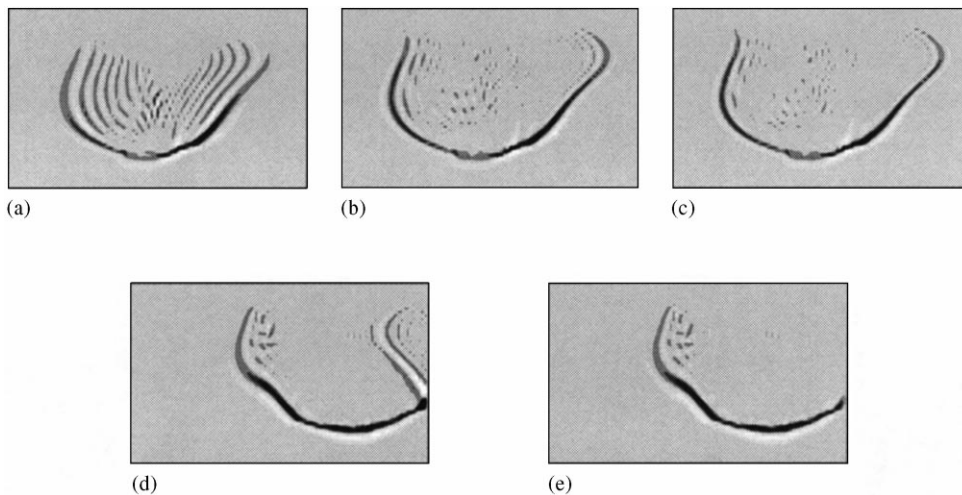


Fig. 6. 2-D smooth heterogeneous medium. Snapshots at  $T_{\text{obs}} = 0.34$  s. (a)  $2x_{\text{class}} - 2z$ ; (b)  $4x_{\text{mod}} - 4z$ ; (c)  $6x_{\text{mod}} - 4z$ ; (d) Dirichlet BC,  $4x_{\text{mod}} - 4z$ ; (e) PLMS of  $5 \Delta x$ ,  $4x_{\text{mod}} - 4z$ .

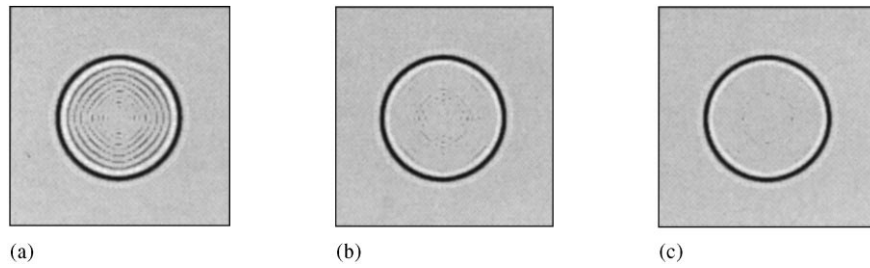


Fig. 7. 3-D homogeneous medium. Snapshots at  $z_{\text{obs}} = 375$  m and  $T_{\text{obs}} = 0.51$  s. (a)  $2x_{\text{class}} - 2z$ ; (b)  $4x_{\text{mod}} - 2z$ ; (c)  $6x_{\text{mod}} - 4z$ .

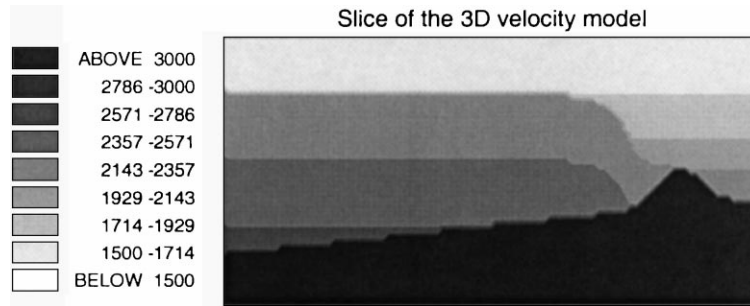


Fig. 8. An  $(x, z)$  slice of a 3-D smooth heterogeneous medium; level lines of the velocity.

wavelength for  $F_S$ . The results in Fig. 6 represent the solution at time  $T_{\text{obs}} = 0.34$  s. In the first experiment, the point source is located in the center of the domain. Figs. 6(a)–(c) show that the modified schemes give very good results, in heterogeneous media, and a very good improvement concerning the dispersion, compared to the second-order scheme. The second experiment is devoted to testing the PML absorbing boundaries described in Section 2.2. We

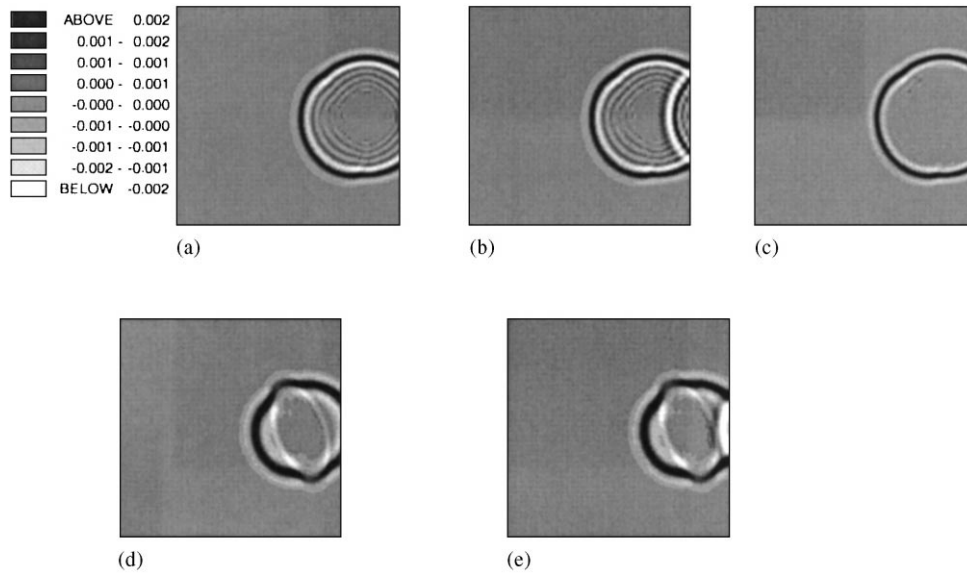


Fig. 9. 3-D heterogeneous medium. Sections of snapshots at  $T_{\text{obs}} = 0.254$  s. (a)  $z_{\text{obs}} = 20, 4x_{\text{mod}} - 2z$  (Claerbout) with PMLs of  $6 \Delta x$ ; (b)  $z_{\text{obs}} = 20, 4x_{\text{mod}} - 2z$  with Dirichlet BC; (c)  $z_{\text{obs}} = 20, 6x_{\text{mod}} - 4z$  with PMLs of  $6 \Delta x$ ; (d)  $z_{\text{obs}} = 30, 4x_{\text{mod}} - 2z$  with PMLs of  $6 \Delta x$ ; (e)  $z_{\text{obs}} = 30, 4x_{\text{mod}} - 2z$  with Dirichlet BC.

shift the location of the source close to the left boundary of the domain and present the results obtained with scheme  $4x_{\text{mod}} - 4z$ . The strong reflection obtained with a Dirichlet boundary condition shown in Fig. 6 (d) has completely disappeared with an absorbing layer of depth  $5h$  shown in Fig. 6(e). This illustrates the capacity of the PML in heterogeneous media. The extra cost due to the PML is negligible as the layer represents 5% of the total length.

### 5.2. Filtered point source in a 3-D homogeneous medium

This simulation is performed in a 3-D homogeneous medium with  $c = 1000$  m/s. We consider a filtered point source. The difference from the 2-D case comes from the inverse Fourier transform,  $\mathcal{F}_{x_1, x_2}^{-1}(1_{|ck| < |\omega|})(x_1, x_2) = |\omega|/|2\pi cx|J_1(|\omega x|/c)$ , where  $J_1$  denotes the Bessel function. The central frequency of the source is  $F_S = 20$  Hz and the cutoff frequency is  $F_C = 50$  Hz. The number of points per wavelength is about 4 for  $F_S$  along the  $x_1$  direction, but only 3 along the diagonal. Fig. 7 shows sections of the solution at a fixed depth  $z_{\text{obs}} = 375$  m observed at time  $T_{\text{obs}} = 0.51$  s. Note the quite good isotropy despite the introduction of particular directions used for the splitting.

### 5.3. Filtered point source in a 3-D heterogeneous medium

The last simulation is performed in a smooth varying velocity medium. A slice of this medium appears in Fig. 8. The number of points per wavelength for the central frequency is about 5 in the  $x$  direction and 3.5 along the diagonal. In Fig. 9, we represent the sections of the solution at time  $T_{\text{obs}} = 0.254$  s for two fixed depth ( $z_{\text{obs}} = 20$  in (a)–(c) and  $z_{\text{obs}} = 30$  in (d) and (e)). The improvement on the dispersion using a higher-order scheme is still very good in this heterogeneous medium (compare Fig. 7(a) and (c)). The PML technique is also used here. Although the extra cost is a bit higher and the absorption with only six layers is not as accurate as in 2-D, the results compared to the Dirichlet BC are still quite good (compare Fig. 7(a) and (b) at  $z_{\text{obs}} = 20$  and Fig. 7(d) and (e) at  $z_{\text{obs}} = 30$ ).

## References

- [1] F. Collino, P. Joly, Splitting of operators, alternate directions and paraxial approximations for the 3-D wave equation, *SIAM J. Sci. Comput.* 16 (1995) 1019–1048.
- [2] F.D. Tappert, The parabolic approximation method, in: J.B. Keller, J.S. Papadakis (Eds.), *Wave Propagation and Underwater Acoustics*, Springer, Berlin, 1977, pp. 224–287.
- [3] F.B. Jensen, W.A. Kuperman, M.B. Porter, H. Schmidt, *Computational Ocean Acoustics*, American Institute of Physics, New York, 1994, pp. 343–412.
- [4] J.F. Claerbout, Coarse grid calculations of waves in inhomogeneous media with application to delineation of complicated seismic structure, *Geophysics* 35 (1988) 407–418.
- [5] J.F. Claerbout, *Fundamentals of Geophysical Data Processing*, McGraw-Hill, New York, 1976.
- [6] D. Hale, Stable explicit depth extrapolation of seismic wave-fields, *Geophysics* 56 (1991) 1770–1777.
- [7] H. Brysk, Numerical analysis of the  $45^\circ$  finite difference equation for migration, *Geophysics* 48 (1983) 532–542.
- [8] P. Joly, M. Kern, Numerical methods for 3-D migration, Annual Report, PSI Consortium, 1990.
- [9] M. Kern, A nonsplit 3D migration algorithm, in: S. Hassanzadeh (Ed.), *Proceedings of Mathematical Methods in Geophysics Imaging III*, SPIE, 1995.
- [10] D.L. Brown, Applications of operator separation in reflection seismology, *Geophysics* 3 (1983) 288–294.
- [11] R.W. Graves, R.W. Clayton, Modeling acoustic waves with paraxial extrapolators, *Geophysics* 55 (1990) 306–319.
- [12] D. Ristow, T.D. Ruhl, 3-D implicit finite-difference migration by multiway splitting, *Geophysics* 62 (1997) 554–567.
- [13] F. Collino, Numerical analysis of mathematical models for wave propagation, PSI Consortium Report, 1993.
- [14] G. Marchuk, Splitting and alternating direction methods, in: *Handbook of Numerical Analysis I*, Elsevier, Amsterdam, 1994.
- [15] A. Bamberger, B. Engquist, L. Halpern, P. Joly, Paraxial approximations in heterogeneous media, *SIAM J. Appl. Math.* 48 (1988) 98–128.
- [16] M.D. Collins, E.K. Westwood, A higher-order, energy-conserving parabolic equation for range-dependent depth, sound speed, and density, *J. Acoust. Soc. Amer.* 89 (1988) 1068–1075.
- [17] M.D. Collins, W.L. Siegmund, A complete energy conservation correction for the elastic parabolic equation, *J. Acoust. Soc. Amer.* 105 (1999) 687–692.
- [18] J.P. Béranger, A perfectly matched layer for the absorption of electromagnetic waves, *J. Comput. Phys.* 114 (1994) 185–200.

- [19] F. Collino, Perfectly matched absorbing layers for the paraxial equations, *J. Comput. Phys.* 131 (1997) 164–180.
- [20] E. Bécache, F. Collino, P. Joly, Higher-order numerical schemes and operator splitting for solving 3D paraxial wave equations in heterogeneous media, INRIA Report 3497, 1998.
- [21] G.D. Akrivis, V.A. Dougalis, N.A. Kampanis, Error estimates for finite-element methods for a wide-angle parabolic equation, *Appl. Numer. Math.* 16 (1994) 81–100.
- [22] N. Tordjman, *Eléments finis d'ordre élevé avec condensation de masse pour l'équation des ondes*, Ph.D. Thesis, University of Paris IX, 1995.